



Comparison of downstream scour of single and combined free-fall jets in co-axial and non-axial modes

Atoosa Latifi¹ · Seyed Abbas Hosseini¹  · Mojtaba Saneie²

Received: 28 April 2018 / Accepted: 9 July 2018 / Published online: 25 July 2018
© Springer Nature Switzerland AG 2018

Abstract

Downstream plunge pools of dams have been exposed to erosion caused by falling jets of the hydraulic structure's outlets. This damages the foundation and body of the dam and its constituent structures. Therefore, investigating the scouring phenomenon of plunge pools is one of the important issues in hydraulic engineering. The present research investigates the characteristics of scour holes by single jets and combined jets in different operational modes of dam spillway and outlet. Using experimental modeling, 36 experiments were conducted with various discharges and two tail water depths in single and combined jet modes. The results show that combined jet has lower scour depth and hill height than single jets in all conditions. Comparing the depth and length of the hole and hill height caused by scouring reveals that combined jet is approximately between 5 and 10% greater for a co-axial than for non-axial combined jets in all tail water conditions. But the width of the scour hole of the non-axial combined jets is more than the co-axial one. With the aid of dimensional analysis, an equation is proposed for calculating the scouring characteristics of the combined jets, which is a good determination coefficient between calculated and observational data. Also, the dimensionless results show that the length of the scour hole and the length of mound are about one and a half times the position where the maximum scour depth is formed. Thus, a unit non-dimensional curve can be obtained for the longitudinal profile of scour. The results of the study indicate that, given the case of combining jets as non-axial, the depth and length of the scour holes are lower than the single mode, and that downstream scour can be controlled and reduced relative to the co-axial state by combining the non-axial spillway outlet jet with the orifice jet.

Keywords Single jet · Combined jets · Plunge pool · Scour hole

Introduction

One of the important issues in the design of dams and hydraulic structures is the transfer of water downstream in rivers without causing severe damage to the environment and the destruction of these structures. Spillway and outlets are the most important hydraulic structures for flood flow

because jets can cause damage due to of the high flow velocity. Hence, their energy should be greatly dissipated.

Scouring is a dynamic process between air, water, and sediment. Empirical studies show that the collision of the water jet with downstream flow creates erosion in the alluvial bed: this, consequently, causes scouring and transports sediments downstream. Over time, the turbulence intensity of the flow and the shear stress produced in the bed decreases and a scouring hole is formed.

The scour hole is affected by parameters such as the jet outlet flow characteristics and the geometry of the hydraulic structure. A lot of research has been done in the past few years on the geometric properties of scour holes for single impact jets. Investigations show that the scouring process depends on various parameters, such as outlet jet discharge, Froude number, jet air mixing, tail water and sediment characteristics (Mih and Kabir 1983; Farhoudi and Smith 1985; Aderibigbe and Rajaratnam 1996; Canepa and Hager 2003; Pagliara et al. 2006). The results of the

✉ Seyed Abbas Hosseini
abbas_hoseyni@srbiau.ac.ir

Atoosa Latifi
atoosa_latifi@yahoo.com

Mojtaba Saneie
saneie_m@scwmri.ac.ir

¹ Department of Civil Engineering, Science and Research Branch, Islamic Azad University, Tehran, Iran

² Soil Conservation and Watershed Management Research Institute, Tehran, Iran

studies by these researchers confirm that with increase in the discharge and Froude number, the rate of scour increases, and as the jet air mixing and tail water increase, the scour quantity decreases.

Pagliara et al. (2006) indicated that the sediment formed after the scour hole plays a major role in limiting the development of the scour hole before it and the scour hole does not expand much with increase in the height and volume of the sediment. Almeida Manso (2006) showed that scouring is a function of the jet type and the length of the jet trajectory, the discharge, the tail water, and type of the material and sediment of the downstream bed. Many researchers such as Veronese (1937), Chee and Kung (1974), Khatsuria (2004) and Azmathullah et al. (2006) have proposed a general form of Eq. (1) to estimate the scour depth downstream of free-fall jets. In Eq. (1), q is the discharge per width, H is jet falling height, α is jet collision angle, and d is the diameter of the bed material. As can be seen, with increase of the discharge and the height of the jet falling, the dimensions of the scour hole also increase:

$$d_s = \frac{cq^x H^y \alpha^w}{d^z}. \quad (1)$$

Considering the extensive research on single jet and scouring mechanisms, the investigations on combining free-fall jets are limited. Investigating the scouring of multiple jets is a complex phenomenon and many parameters can affect it: this is why it is not an easy task to estimate scouring in this case. Few studies have been conducted on multiple jets. The practical application of multiple jets can be described in some cases in concrete dams with two or more outlets or jet outlets from spillway and orifice that are combined at the same time.

Negam (1995) analyzed the characteristics of the combination flow over the spillway and through the bottom of the rectangular gate with unequal geometric shapes. Uyumaz (1988) studied the downstream scour hole as a result of the flow passing through a gate and compared it with single jet mode over the gate. He proposed an equation for estimating the scour depth with two types of sediment: this demonstrated that the maximum scour depth of jets over the gate is more than at the bottom of the gate. Dehghani et al. (2010) conducted an experimental studies of the downstream scour hole of a jet passing over and under a gate and combining jets at the same time. They concluded that the maximum scour depth depends on the channel geometry, the distance between the gate and the spillway, the opening percentage and the water head on the spillway, particle diameter, particle density, bed slope, viscosity, gravity acceleration, discharge, velocity, and the depth of water upstream of gate. The results of their experiments showed that the maximum scour depth in the

jet passing over the spillway is greater than the combined jet and the jet passing through the bottom of gate under the same conditions.

Pagliara et al. (2011) compared the downstream scour of two symmetric crossing jets with a single jet. They conducted their experiments with the angle variations between the two crossing jets, Froude number, and tail water changes. It was concluded that increase in the angle between the crossing jets and increase in the tail water reduces the depth of the scour hole. Also, with the increase in the Froude number, the depth of the scour hole increases: and under the same conditions, the depth of the scour hole in crossing jets is lower than single jets.

Mehraein (2012) studied the downstream scour of the crossing wall jets with the circular cross section. Their observation showed that the scour hole has had two parts: the first portion is the scour caused by a single wall jet and the second scour is caused by the second wall jet impacting the first jet with a 90° angle. They showed that the two maximum scour depths from a single and crossing jet depend on Froude number of the single jet, Froude number of the crossing jets, the tail water, and the horizontal distance between the crossing jets of the wall jet. They proposed a non-dimensional equation for the scour depth that included the Froude number of the single jet, Froude number of the crossing jets, and the tail water. The results of the study showed that with increase in the tail water and increase in the horizontal distance between the crossing jets of the first wall jet, the scour depth decreases and the length of the scour hole and the horizontal distance between the sediment and the first wall jet increases. Pagliara and Palermo (2017) carried out an experimental study on non-crossing jets with variations in tail water, discharge rate, crossing angle, and crossing location of jets in terms of the channel bed. The effect of the crossing location of jets relative to the channel bed was considered an important parameter: if this distance is greater than a certain amount, the jets do not collide and act like two single jets.

Reviewing these previous studies, it seems that despite extensive research on the falling single-jet scouring mechanism, there is very limited work on the effect of the scouring mechanism on the impact of simultaneous and combined jet operations. Therefore, this research investigates scouring mechanism in the case of the combination of jets in co-axial and non-axial modes. This is mainly the case in concrete dams where the spillway outlet jet operates simultaneously with the bottom outlet jet: by opening one of the gates of the dams, the combination of jets can be viewed in a co-axial or non-axial manner. Therefore, the downstream scouring of the dam in case of occurrence of any of the above conditions is necessary. Given the possibility of maneuvering over the operation and releasing the flood from the spillway and bottom outlet that acts as an orifice, this study seeks to

examine how to control and reduce the rate and manner of the scour hole by the method of combining spillway and orifice outlet jets.

Data base and methodology

Experiments were conducted at the Hydraulic Laboratory of Iran, Water Research Center: 36 experiments were carried out in a 7-m plunge pool, 6.5 m wide and 1.1 m high. A bed channel with 0.9 m depth of uniform sediments was made of coarse gravel with a mean diameter of $d_{50} = 15$ mm, a density of 2.65 g/cm^3 , and a standard deviation of 1.10 which was horizontally covered. There was a sliding gate at the end of the channel that controlled the tail water. The model had a water supply system consisting of two centrifuge pumps and pipes with associated connections for controlling discharge rate. Flow through the pipes first entered the reservoir’s canal and then the reservoir through a metal screen: this occurred after the loss of surface turbulence. The upstream reservoir was 6.8 m in length, 6.5 m in width, and 4 m in height. Flow through the input channel entered the spillway approach channel. The spillway was made of transparent plexiglas and had three gates with three spans: after passing through the spillway, the flow entered a chute with a constant slope of 16% and was finally thrown downstream by a flip-bucket with a 25° angle. The flip-bucket had three equal rectangular spans with cross sections of 22 cm width. The flip-bucket level was 1.45 m above the bottom of the plunge pool. To create the second jet, an orifice with rectangular cross section and dimensions of $11 \times 11 \text{ cm}^2$ was used in the dam body. The orifice had been installed under the flip-bucket in a co-axial with the second span of spillway at a level of 26 cm from the plunge pool bottom and co-axial. Orifice outlet had a flip bucket structure at the end, which provided a free-fall jet. In order to observe the flow pattern, the orifice was made of transparent plexiglas. To control and adjust the output flow, a butterfly gate was installed on the orifice. The flow was unevenly distributed between the spillway and the bottom outlet. The tail water and inlet discharge rates were regulated and measured by a rectangular spillway located at the bottom of the channel. The specification and experimental layout have been shown in Fig. 1. The equilibrium time of the runs when the scouring hole reached to equilibrium was based on the evidence experiment: it was 2 h. Tests were carried out for up to 7 h to ensure that the tests reached the time of relative equilibrium. The discharge was stopped after the equilibrium time: when the hole was drained, the maximum scour depth, length, and width of the hole and scouring pattern were then taken in three dimensions. Laser meter was used for three-dimensional survey of the scour hole. For this purpose, a fixed frame 2.5 m in length and 4 m in width was used: its length and width were

divided into a 20 cm mesh and moving rails equipped with laser meters. In this condition, x , y , and z of each point of the scour hole was measured. After completing each run, the pump was shut off, the hydraulic conditions regulated, and the bed flattened for subsequent experiments. Figure 1b, c show the overall scouring scheme and plunge pool.

In Fig. 1, Z_m : maximum scour depth; Z_M : maximum hill depth after scour hole; L_m : the length corresponding to the maximum scour depth; L_a : scour hole length; L_M : the length corresponding to the maximum hill depth after the scour hole; L_b : the total length of the scour hole and subsequent sedimentation; W_m : maximum scour width; Q_s : discharge spillway; Q_o : orifice discharge rate; h_o : tail water; H : water height in the reservoir.

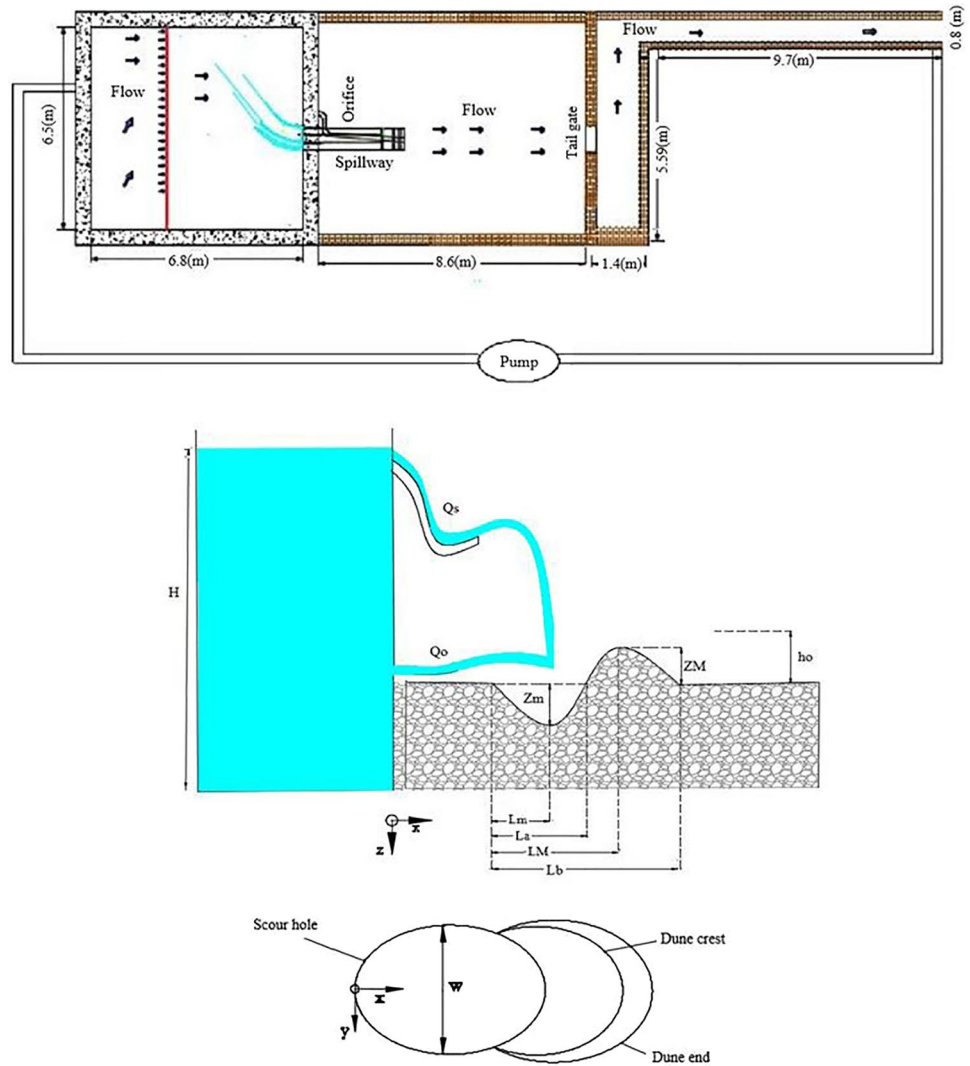
36 experiments were carried out in accordance with different hydraulic conditions in single jet and combined jet modes. The first mode of the experiments was conducted with discharge rates of 26, 36, and 54 l/s passing through spillway gates. These spillway gates were called S(1), S(2), and S(3) from left to right respectively, where S(2) was co-axial with orifice or bottom outlet. The flow passed through the spillway gates to the flip-bucket and formed a falling jet. The second mode of the experiments was performed at different discharge rates of $Q = 26, 36, \text{ and } 54 \text{ l/s}$ for spillway, as in the first case, and combined with a constant discharge rate of orifice of $Q = 18 \text{ l/s}$ S(1)+O:S(3)+O was non-axial combined jet and S(2)+O was co-axial combined jet. It should be noted that spillway discharges were 1.5, 2, and 3 times the orifice discharge rate in the experiments. All combined and single jet tests were performed for two tail waters of 5 cm and 8 cm.

If ϕ is the characteristic of the scour hole, which includes the maximum scour depth Z_m , the maximum length of the scour hole L_m , and the scour hole width W_m , it can be written that:

$$\phi = f(Q_s, Q_o, Q_i, V_s, V_o, V_i, \mu, Y_t, d_{50}, g, \rho_s, \rho_w, R, \cos\theta, Y_o, Y_s, h_f, h_o, H). \tag{2}$$

In Eq. (2), Q_s is the spillway discharge (l/s), Q_o is the orifice discharge (l/s), Q_i is the flow rate of combined jets (l/s), V_s is the spillway jet velocity at the lip of the flip-bucket of spillway (m/s), V_o is the jet velocity at the lip of the orifice flip-bucket (m/s), V_i is the vector summation of combined jet velocity (m/s), d_{50} is the median diameter of bed material (mm), θ is the flip-bucket angle, g is the gravity acceleration (m/s^2), ρ_s is the bed sediment density (kg/m^3), ρ_w is the water density (kg/m^3), μ is the dynamic water viscosity (N m/s), Y_t is tail water (m), Y_s is the depth of water over the spillway flip-bucket (m), Y_o is the depth of water on the orifice flip-bucket (m), H is water height in the reservoir (m), h_f is the vertical distance between the edge of the flip-bucket of spillway and the bed surface of the plunge pool (m), h_o is

Fig. 1 Plan, sections, of the experimental set up



the vertical distance between the edge of the flip-bucket of orifice and the bed surface of the plunge pool (m), and R is the hydraulic radius of the spillway flip-bucket (m).

Equation (3) was obtained using the Buckingham theory, by eliminating constant values—including h_f , h_o , θ , and R —in the course of the experiments of this research, and by neglecting μ or the dynamic water viscosity Reynolds number due to turbulence and its ineffectiveness on the scour characteristic (Dehghani et al. 2010; Mehraein 2012; Pagliara et al. 2011; Pagliara and Palermo 2017):

$$\frac{\phi}{H} = f\left(Fr_s, Fr_i, \frac{Y_t}{H}\right). \quad (3)$$

In Eq. (3), $Fr_s = V_s / \left[gd_{50}(\rho_s - \rho_w)d_{50}/\rho_w\right]^{0.5}$ is the Jet densimetric Froude number caused by the spillway falling jet, $V_i = (V_s^2 + V_o^2)^{0.5}$ is the resultant velocity of the combined jets, $Fr_i = V_i / \left[gd_{50}(\rho_s - \rho_w)d_{50}/\rho_w\right]^{0.5}$ is the Jet den-

simetric Froude number of the spillway and orifice combined jets, and ϕ is the scour characteristic including the depth, maximum length, and width of the scouring.

Results and discussion

Scouring was observed at the beginning of the experiments and when the falling jets collided with the bed of the plunge pool. With the onset of scouring, the bed material was removed from its place and came to the surface: it got randomly distributed due to the vortices created in the plunge pool. The scouring hole was also formed by the onset of this phenomenon, which caused the eroded materials to move downstream. They were deposited by weight and according to the size and diameter of the materials. As time went on, the depth of the hole increased and the hill depth increased afterwards. The hill created at the front of the hole prevented

particle output by acting like a barrier and making it difficult for them to exit. In this case, the particles must travel a long way to exit the hole. The experiments continue until the other particles cannot escape from the hole: this occurs during the test's equilibrium time of 2 h in the evidence run. At this equilibrium time, the particles inside the hole are spinning due to vortexes. By stopping the flow at equilibrium time, suspended particles are deposited in the hole under the influence of their weight and a hole with a hill in front is created. Table 1 presents a summary of the results of the experiments, including the scour hole depth and the hill height.

Scour hole depth

One of the most important scour parameters is the maximum depth of the scour hole and the height of the hill. In Fig. 2, the maximum scour depth and subsequent hill for single jet modes' output from spillway gates S(1), S(2), and S(3) and combined jets of the first and the third spillway spans in non-axial form with an outlet orifice jet S(1)+O and S(3)+O and the combined jet of the second spillway span co-axial with orifice jet S(2)+O have been compared at two dimensionless tail waters (Yt/H)=0.02, 0.04. In general, the results show that the maximum scour depth and sediment height increases with increase in the Jet densimetric

Table 1 Presents a summary of the results

Definition	Q _s (l/s)	Q _o (l/s)	fr	Z _m (cm)	Z _M (cm)	L _m (cm)	L _a (cm)	L _M (cm)	L _b (cm)	W (cm)
S1 Yt/H=0.02	26	0	4	23.5	18	133	195	255	385	140
	36	0	5.2	28.5	23	148	220	285	415	160
	54	0	7	36.5	31	173	245	315	455	180
S2 Yt/H=0.02	26	0	4	24	19	135	200	260	390	135
	36	0	5.2	29.1	24	150	225	290	420	155
	54	0	7	37	32	175	250	320	460	175
S3 Yt/H=0.02	26	0	4	23	17	131	190	250	380	137
	36	0	5.2	28	22	146	215	280	410	157
	54	0	7	36	30	171	240	310	450	177
S1 Yt/H=0.04	26	0	4.0	19.5	12	118	155	215	345	120
	36	0	5.2	23.6	16	135	185	245	375	140
	54	0	7	31	22	160	215	275	415	165
S2 Yt/H=0.04	26	0	4.0	20	13	120	160	220	350	115
	36	0	5.2	24.1	17	137	190	250	380	135
	54	0	7	31.5	23	162	220	280	420	160
S3 Yt/H=0.04	26	0	4	19	11	116	150	210	340	117
	36	0	5.2	23	15	132	180	240	370	137
	54	0	7	30.5	21	157	210	270	410	162
S1+O Yt/H=0.02	26	18	6	28	21	148	210	275	400	170
	36	18	7.5	34	27	165	235	305	440	190
	54	18	9	41	34	187	260	340	480	210
S2+O Yt/H=0.02	26	18	6	29.5	24	160	240	300	440	150
	36	18	7.5	36.1	30	180	260	335	475	170
	54	18	9	44.1	37	200	280	370	510	190
S3+O Yt/H=0.02	26	18	6	27.5	20	150	205	270	395	167
	36	18	7.5	33.5	26	168	230	300	435	187
	54	18	9	40.5	33	190	255	335	475	205
S1+O Yt/H=0.04	26	18	6	24	14	127	170	220	350	140
	36	18	7.5	30	19	147	195	250	390	160
	54	18	9	37	25	167	220	290	430	180
S2+O Yt/H=0.04	26	18	6	25	16	135	180	235	370	120
	36	18	7.5	31	21	155	205	270	405	140
	54	18	9	38.1	27	175	230	310	450	160
S3+O Yt/H=0.04	26	18	6	23.5	13	130	165	215	345	135
	36	18	7.5	29	18	150	190	245	385	155
	54	18	9	36.5	24	170	215	285	425	175

Froude number. Similar results have been observed in previous investigations (Dehghani et al. 2010; Mehraein 2012; Pagliara et al. 2011; Pagliara and Palermo 2017).

It can be seen in Fig. 2a, b that in the combination of jets in co-axial mode or S(2)+O, the maximum scour depth and hill is more than the combination of jets in the non-axial mode. The results also show that with increase in tail water for both single jet and combined jet, scour depth decreases. One of the significant results in Fig. 2a, b is that the distribution of the outflow from the dam between the orifice and the spillway has lesser scour depth than the state in which the entire outflow is through the spillway. The main reason for this is the interference between two jets and the reduction of the energy output of the jets relative to the condition where a single jet falls downstream.

With regard to the ratio of discharge rates considered in this study for spillway and orifice, the discharge of jet of the spillway outlet relative to the orifice ranges from about $Q_s/Q_o = 1.5$ to a range of $Q_s/Q_o = 2-3$. In the co-axial mode, the combined jets were observed for all discharge ratios tested in this study so that the two jets appear completely mixed together and a vortex is formed in the scouring hole. In other words, because the axis of the orifice is exactly co-axial with the spillway axis at span no. 2 and the spillway outlet jet interferes with the orifice jet even as it reduces the output jet energy, it creates a single vortex in the scouring hole whose erosion power is less than the vortex formed by a single jet and higher than the vortex associated with non-axial jets. Therefore, the maximum depth of the scour hole and hill after that are lower than single jet in the same conditions and more than the non-axial combined jet. But in the case of non-axial jets, or S(1)+O and S(3)+O, the jet of spillway outlet has the least interference: in the scour hole, it creates vortexes in the opposite direction. Therefore, the effect

of reduction on the downstream scouring hole is observed in this state. It should be noted that due to the positional symmetry of gates 1 and 3, the maximum scour depth and hill in these two states is almost equal to the combination of the orifice jet. On the other hand, the same applies to the spillway jets without the orifice function: the maximum scour depth and hill for the spillway spans 1, 2, and 3 are roughly equal due to equal flow rates and the same geometric characteristics.

The effect of tail water on changes in the maximum depth of the scour hole for the states S(1), S(1)+O, S(2), S(2)+O, S(3), S(3)+O in Fig. 2 shows that with increase in tail water, the maximum depth of the scouring hole gets reduced. This is also evident in previous researches: the reason is that by increasing the tail water, an elastic cushion is formed on the surface of the plunge pool which plays a dissipating role in the energy of the crossing jets (Pagliara et al. 2006, 2011; Sui et al. 2008; Rajaratnam and Berry 1977; Mehraein 2012).

An important issue in single and combined jets is to determine an equation for calculating non-dimensional scour depth. According to Eq. (3), jet densimetric Froude number and tail water can affect the scour characteristics. Accordingly, a general form of Eq. (3) is proposed for determining the scour depth, where A is a coefficient, and B and C are power. For single jet and combined jet, Eq. (3) can be obtained separately from the experimental data of this study as follows:

$$\frac{z_m}{H} = A(Fr)^B \left(\frac{Y_t}{H} \right)^C$$

Based on this and through linear regression, coefficient A and powers B and C were calculated for single jet and combined jet. Equation (4) was obtained for single jet and Eq. (5) for combined jet.

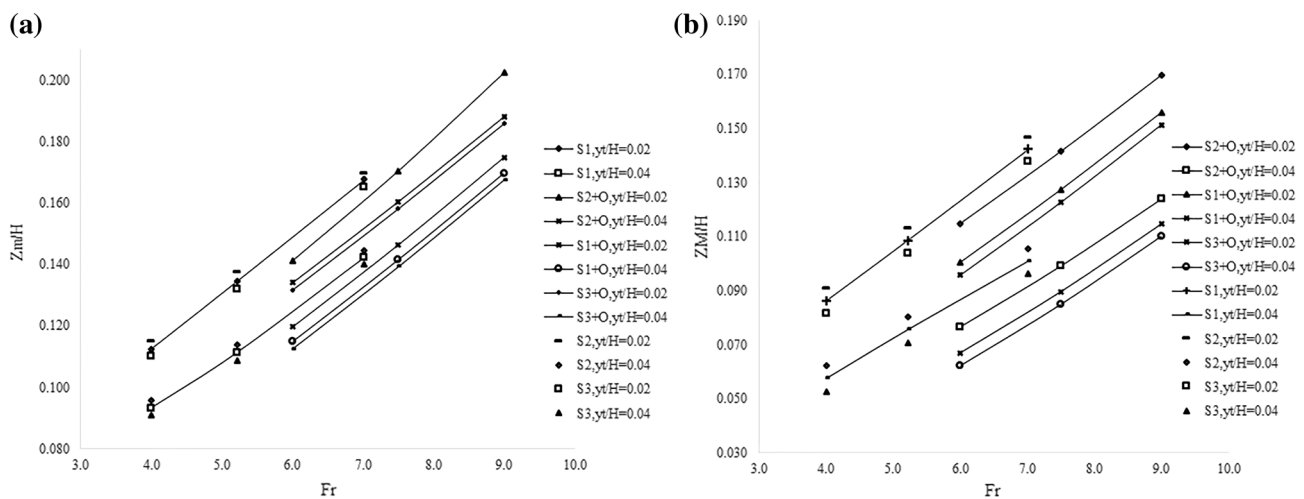


Fig. 2 a Comparison of non-dimensional maximum scour hole depth. b Maximum ridge depth, with Fr for single jet and combined non-axial jet

Non-dimensional equation of maximum scour depth for single jets:

$$\frac{z_m}{H} = 0.012(Fr_f)^{0.8} \left(\frac{Y_t}{H}\right)^{-0.25} \quad R^2 = 0.98. \quad (4)$$

Non-dimensional equation of maximum scour depth for combined jets:

$$\frac{z_m}{H} = 0.012(Fr_f)^{0.91} \left(\frac{Y_t}{H}\right)^{-0.18} \quad R^2 = 0.96. \quad (5)$$

Comparison of Eqs. (4) and (5) shows that the coefficient of both equations is the same and the effect of Froude number on increasing the scour depth of combined jet is higher than single jets, while the inverse effect of tail water on reduced scour depth in single jets is higher than the combined jet. Of course, more experiments are needed in order to reach a sure result. In Fig. 3a, z_m calculated from Eq. (4) has been compared for single jets with observational values. The fitted equation correlates well with the maximum calculated, the observational scour depth: scour and the maximum value of the scour hole can thus be predicted well.

In Fig. 3b, z_m calculated by Eq. (5) for combined jets has been compared with observational values. As expected, due to the collapse of the flow pattern in the case of combined jets, the accuracy of the proposed relationship decreased a little even though it was also able to predict scour depth with acceptable accuracy.

Scour hole length and width

The length of the scour hole is one of the most important parameters because the proximity of the location of the

maximum scour depth compared to the structure can cause its destruction. In combined jets, the length of the scour hole is heavily influenced by how the jets are mixed together.

In Fig. 4a, b, the maximum changes in the scour length L_m and the maximum variation in the width of the scour hole W_m for single jets or S(1), S(2), and S(3) and co-axial combined jets S(2)+O and the non-axial combined jets S(1)+O and S(3)+O have been shown for different Froude numbers and two dimensionless tail water $(Y_t/H)=0.02, 0.04$. This behavior remains almost the same as the scour depth changes. This means that with increase in tail water for both single jets and combined jets, the length and width of the hole decreases, and that with increase in the discharge of falling jets and the consequent increase in the densimetric Froude number, the length of the hole increases.

Regarding the length and width of scour hole, the tail water gave satisfactory results. When the tail water was 0.02, the co-axial combined jet had larger hole length and smaller width than the non-axial one. However, with increase in the tail water, the single jet had higher length and width than the combined jets. Also, in all conditions of tail water, the co-axial combined jet had longer hole length and smaller width compared to a non-axial one. This is due to the interference of the spillway jet and the orifice jet in the co-axial and non-axial conditions. In the case of a non-axial combined jet, two jets maintain some degree of independent behavior and only their vortices in the pool are mixed together. However, for a co-axial jet, the jets are totally overlapping and form a single vortex in the pool.

But in the case of a co-axial combined jet, the tail water behaves differently in comparison to the single jet. This means, the mixing of the orifice jet and spillway jet in a co-axial state would change the crossing angle of jet and increase the length of the scour hole compared to single

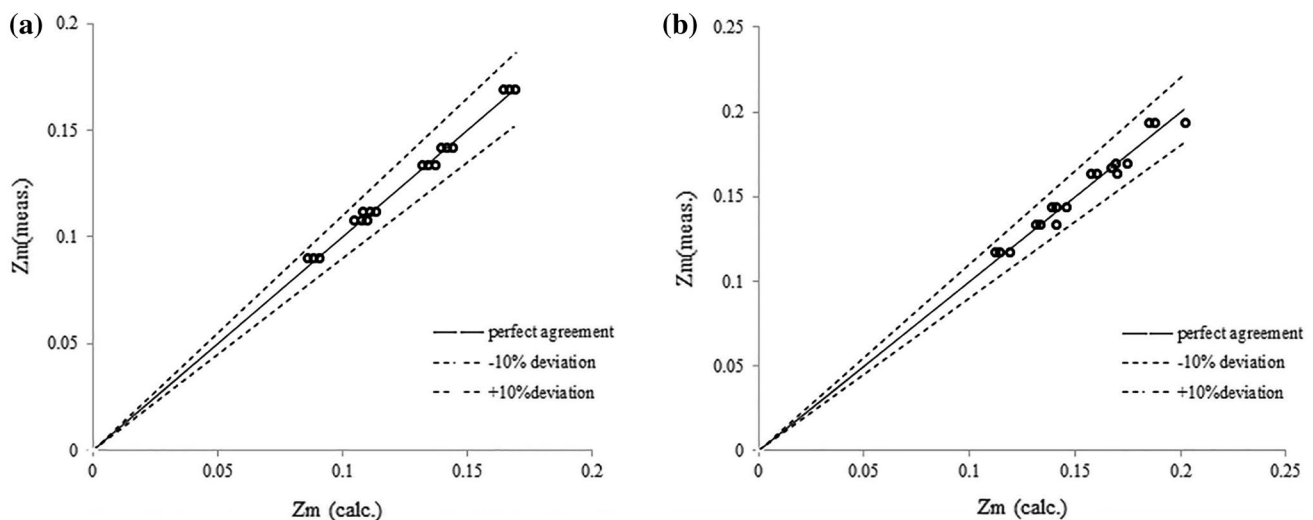


Fig. 3 Comparison of observed (measured) with predicted (calculated) maximum scour depths for: a single jet and b combined jet

jet under similar conditions. However, with increase in tail water, the effect of a single jet on hole length seems greater than the combined jet. Additional experiments with different tail water are needed to make distinct conclusions about this matter and explain this phenomenon.

According to previous studies, similar results have been reported on the effect of the Froude number and also the tail water on the length and width of the scour hole. Given these studies, it is possible to use the proposed relations in the general form of Eq. (3) to calculate the length and width of the hole for a single jet and develop it for a combined jet. Accordingly, with the help of linear regression, coefficient A and powers B and C for single jet and combined jet have been obtained and have been compared in Table 2. According to Table 2, the power associated with tail water and the decreasing effect of tail water on the length and width of the hole in combined jets is more than the single jets.

Comparison of the coefficients of the proposed equation for the length and width of the scour hole shows that these two scour characteristics for single jet and combined jets have the same order of magnitude. Figure 5a shows the comparison of the computational L_m of the equation for single jets, and Fig. 5b shows this comparison for combined jets. As can be seen, the scattering of data for combined jets is higher than for single jets. This is due to the complexity of the behavior and flow pattern in the combined jets as compared to single jets, although the scattering and precision of the combined jet data is also acceptable. The same is holds in Fig. 5c, d on the computational and observational width of the scour hole of single and combined jets.

In Fig. 6, the longitudinal profile of the hole and the hill have been plotted for single and combined jets for dimensionless tail water of $(Y_t/H)=0.02$.

Comparison of scour profiles for single jet and combined jets for dimensionless tail water of 0.02 shows that the shape and profile of scouring in single jet mode has a more regular parabolic shape than the combined jet state: the main reason for this is the interference of vortexes caused by combined jets in the scouring hole and its effect on the curve. Additionally, the development and extension of scour holes and hill will be observed by increasing Froude number.

In Fig. 7, the longitudinal scour profile of S(2)+O and S(1)+O with discharge rate of 36 l/s for spillway jet and discharge rate of 18 l/s for orifice jet has been compared with longitudinal profile of S(2) at discharge rate of 54 l/s for the spillway outlet jet.

It is noteworthy that the longitudinal scour profile and hill in the case where spillway gate 1 operates at discharge rate of 36 l/s and orifice at discharge rate of 18 l/s is slightly less than the longitudinal scour profile and hill of spillway

Table 2 Coefficients A, B, and C and correlation coefficient of non-dimensional equation of maximum scour length and width for single and combined jets

Condition	A	B	C	R ²
Scour length				
Single jet	0.2	0.46	-0.12	0.98
Combined jet	0.14	0.5	-0.18	0.93
Scour width				
Single jet	0.18	0.42	-0.17	0.89
Combined jet	0.11	0.47	-0.26	0.83

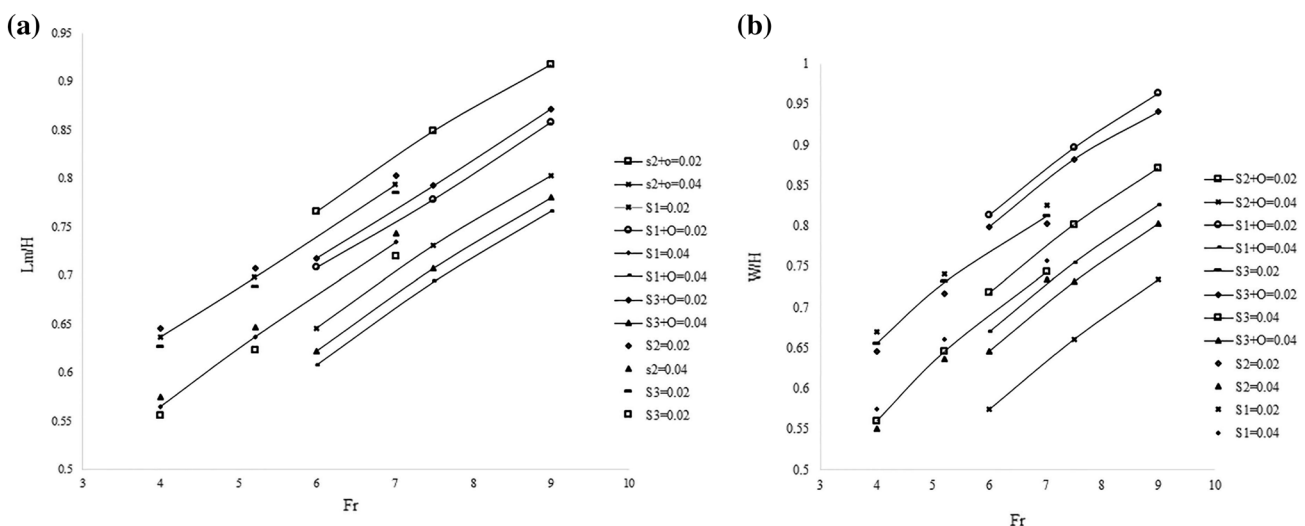


Fig. 4 Dependence of non-dimensional maximum length: **a** dependence of non-dimensional maximum width; **b** with Fr for single jet and combined jet, $\frac{Y_t}{H}$ (0.02–0.04)

gate 2 alone at discharge rate of 54 l/s. Also, the longitudinal scour profile in the case with discharge rate of 36 l/s at gate 2 of spillway with orifice is greater than the longitudinal scour profile for spillway alone with discharge rate of 54 l/s. That is, the co-axial combination of jets increased the depth and length of scour at this discharge rate. This increase includes scour length and hill length. In Fig. 7b, the longitudinal scour profile and dune in the case of gate 1 of spillway with a discharge of 36 l/s and orifice with discharge rate of 18 l/s is less than the longitudinal scour profile and hill of gate 2 of spillway alone with discharge rate of 54 l/s. The longitudinal scour profile in the case of gate 2 of spillway with orifice at discharge rate of 36 l/s is approximately equal to the longitudinal scour profile for spillway alone with discharge rate of 54 l/s. In order to non-dimensionalize the longitudinal scour profiles in all states, the information of the collected data of the depth and length of the scour hole

were non-dimensionalized compared to the maximum depth and scour length.

Figure 8 shows the non-dimensional longitudinal scour profile in all cases and tail waters. The results show that it is possible to propose a general relationship for longitudinal scour profiles independent of the Froude number and tail water. The approximate non-dimensional scour profile can be obtained by measuring the maximum depth and its corresponding length: however, in the deposit area—especially for the combined jet—the scattering of data was much higher. In addition, according to Fig. 8, the length of the hole was about one and a half times the position corresponding with the maximum scour depth and the hill length was about one to one and a half times the depth corresponding to the maximum scour depth. In addition, in combined jets, the total length of the hole and dune was slightly lower.

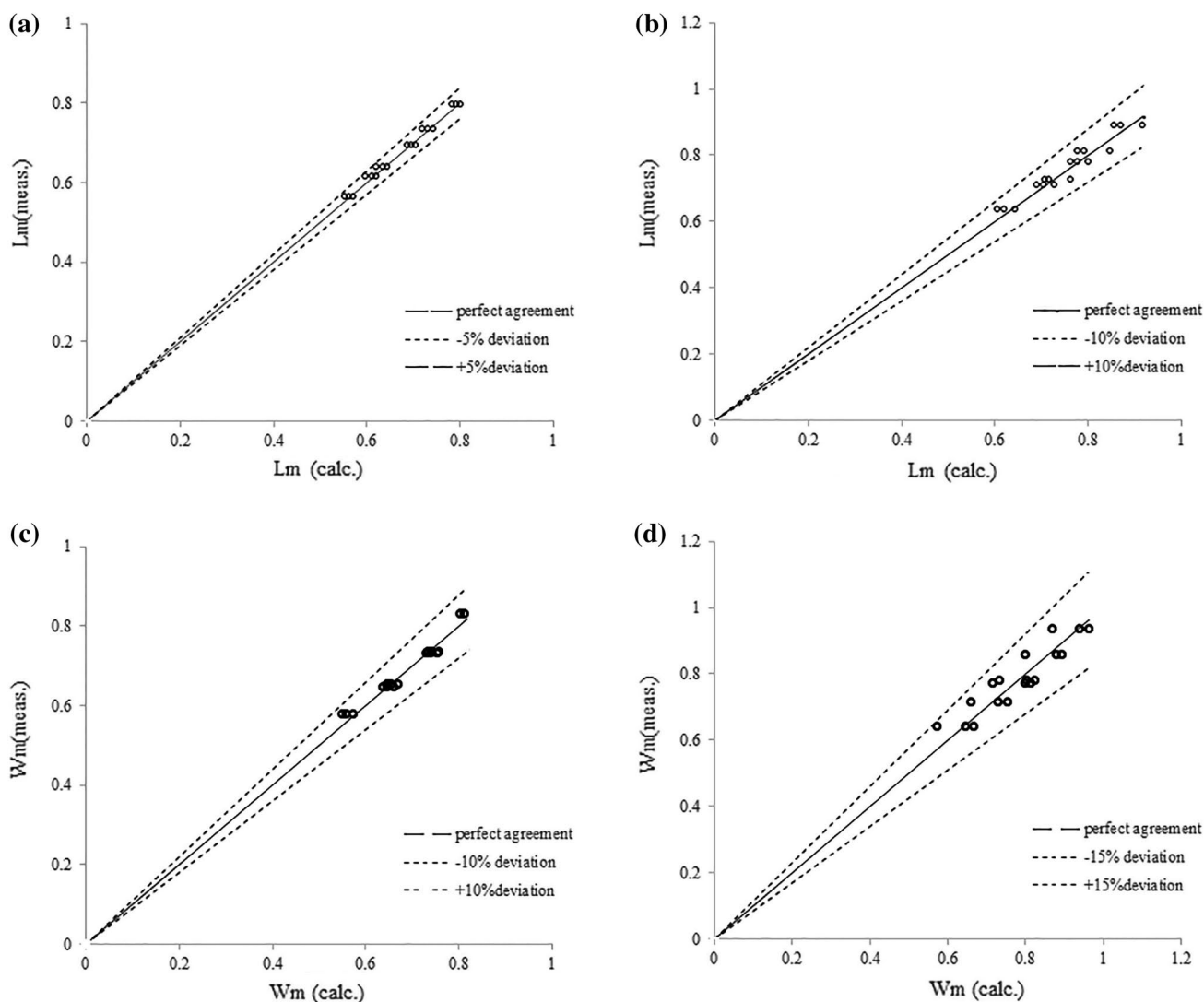


Fig. 5 Comparison between measured and calculated value for: a L_m (single jet); b L_m (combined jet); c W_m (single jet); and d W_m (combined jet)

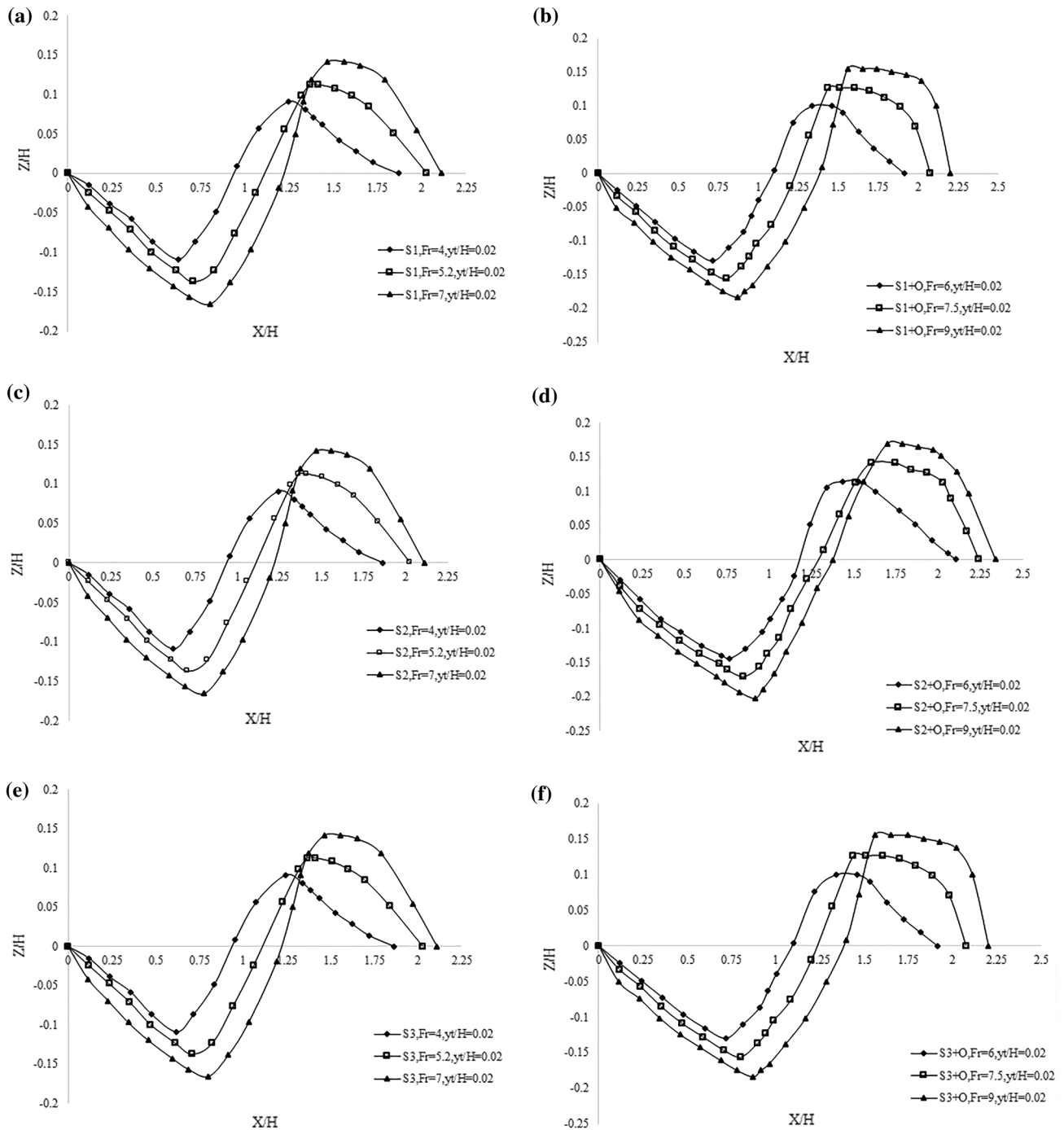


Fig. 6 Longitudinal scour profile: **a** S1; **b** S1 + O; **c** S2; **d** S2 + O; **e** S3; **f** S3 + O. For different Fr with $(Yt/H) = 0.02$

In Fig. 9, the transverse scour hole profile for all modes was plotted for dimensionless tail water $(Yt/H) = 0.02$. The comparison of transverse scour profiles for single and combined jets for dimensionless tail water of 0.02 shows that the scour width of the jet in non-axial combined jets was higher as compared to the co-axial state. The main reason

for this is the interference of vortices caused by non-axial hybrid jets in the scour hole. In addition, the development and extension of scour holes was also seen with increase in the Froude number.

Also, non-dimensional scour profiles for S(1), S(2), and S(3) states were plotted and compared for a given discharge

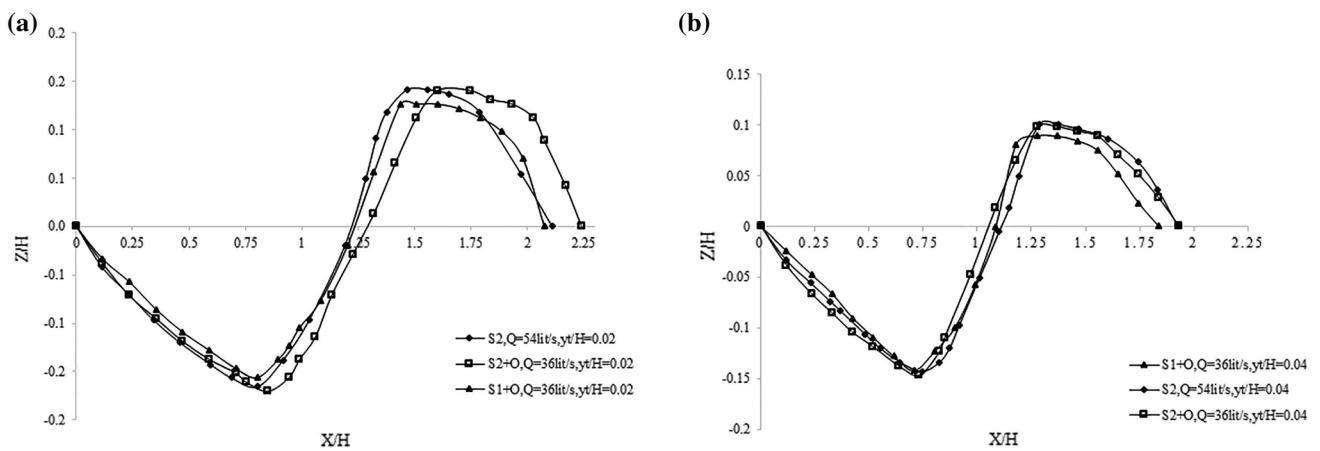


Fig. 7 Comparison of scour profiles for single-jet for spillway discharge 54 l/s, co-axial, non-axial, and combined jets with spillway discharge 36 l/s, and the orifice discharge 18 l/s

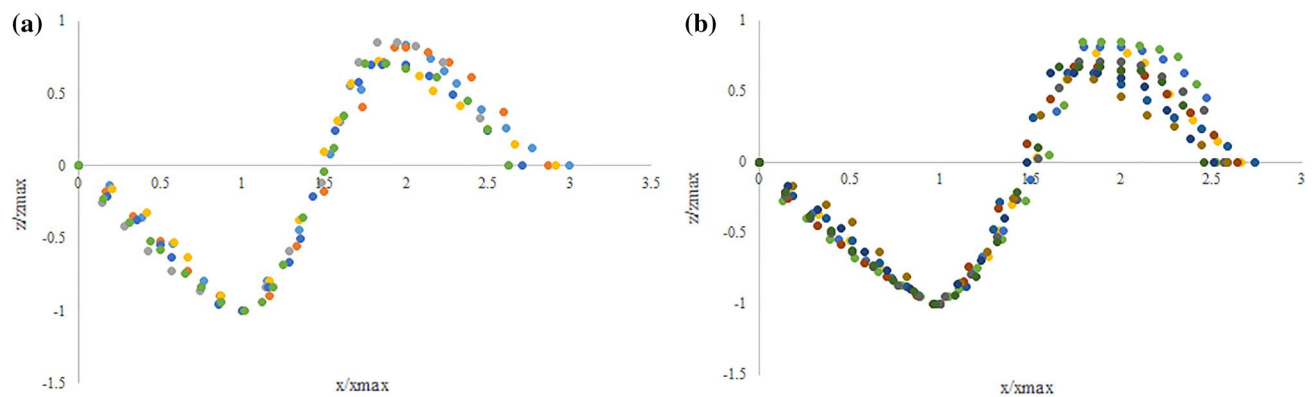


Fig. 8 Non-dimensional longitudinal scour profile for $Yt/H=0.02$: **a** single jet; **b** combined jet

rate of 36 l/s in Fig. 10. The results show that the transverse profile of all three modes for discharge rate of 36 l/s is almost the same. The transverse profile of all three states for other discharge rates is identical. Figure 10a shows the comparison of transverse scour profile for single jets at dimensionless tail water of 0.02, Fig. 10b shows the comparison of transverse scour profile for combined jets at tail water of 0.02, and Fig. 10c shows the comparison of transverse scour profile for combined jets at tail water of 0.04. As can be seen, for non-axial combined jets, the scour width has increased relative to the co-axial state.

Conclusion

Scour caused by dam outlet jets can cause significant damage to the stability of the dam and hydraulic structures. Also, the hydraulic structure’s outlet jet causes the creation of scour hole in the river bed: the depth of this hole will also

change the natural bed of the river, and after the hole there will also be a significant amount of sediment in the river. As a result of the increased scour depth and hill created downstream, the flow encounters an obstacle of sediments and decreases its velocity. Therefore, the equilibrium of sediment transport cycle in the river is altered and the river slope changes, which could create a series of adverse effects in river morphology. Accordingly, the set of measures that can reduce the hole and scour is very important. In flood situations, it is possible to simultaneously exploit the spillway and other outlets. Therefore, conditions for the formation of combined jets are created in the dam downstream. So, in this research, with the help of the experimental model, the performance of combined jets as co-axial and non-axial interference on scour holes was investigated. The results of the research show that:

1. As the densimetric Froude number increases, the maximum scour hole depth will increase. At a given tail

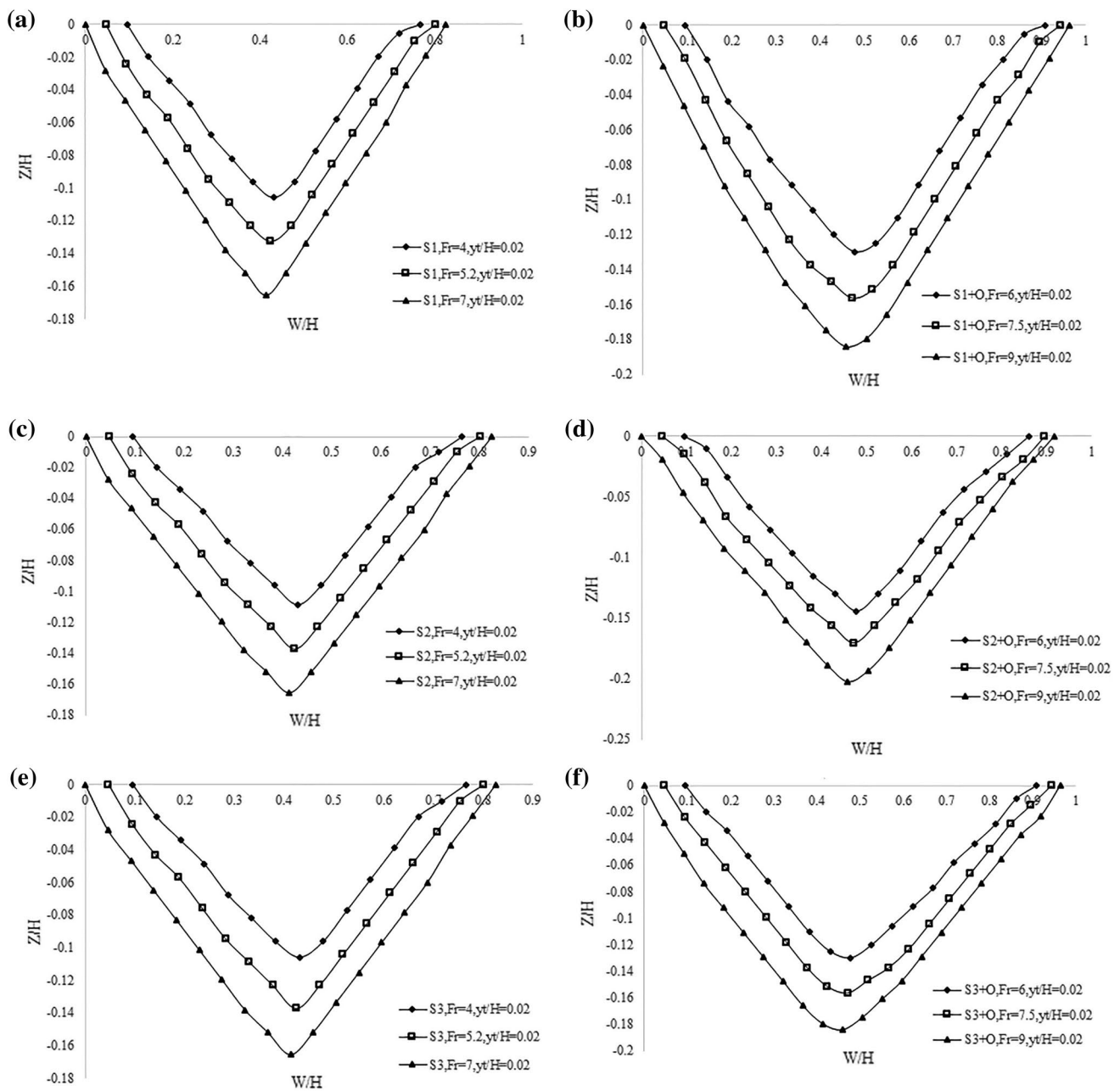


Fig. 9 Transverse scour profile: **a** S1; **b** S1 + O; **c** S2; **d** S2 + O; **e** S3; **f** S3 + O. For different Fr with $(Y_t/H) = 0.02$

water, the maximum scour depth and, consequently, hill in the co-axial hybrid jet of spillway and orifice is higher than the outlet jet in non-axial mode. In addition, due to interference of jets and their energy reduction, the characteristics of scour depth and hill for non-axial combined jets are due to the division of the discharge between the spillway and the orifice less than the single jet with the same discharge rate. This is due to the interference of the spillway jet and the orifice jet in the co-axial and non-axial conditions. As in non-axial combined jet, two jets maintain independent behavior

to some extent and only their vortexes in the pool are mixed together. However, for co-axial jet, the jets are totally interfered and form a single vortex in the pool.

2. The combination of an orifice jet and spillway jet will change the jet angle: though this increases the length of the scour hole, it reduces the scour width. However, with increase in tail water, the jet angle change has no effect on the length of the scour hole. In all conditions, the tail water of non-axial combined jets has a lower hole length and greater scour width. A more complete review of this

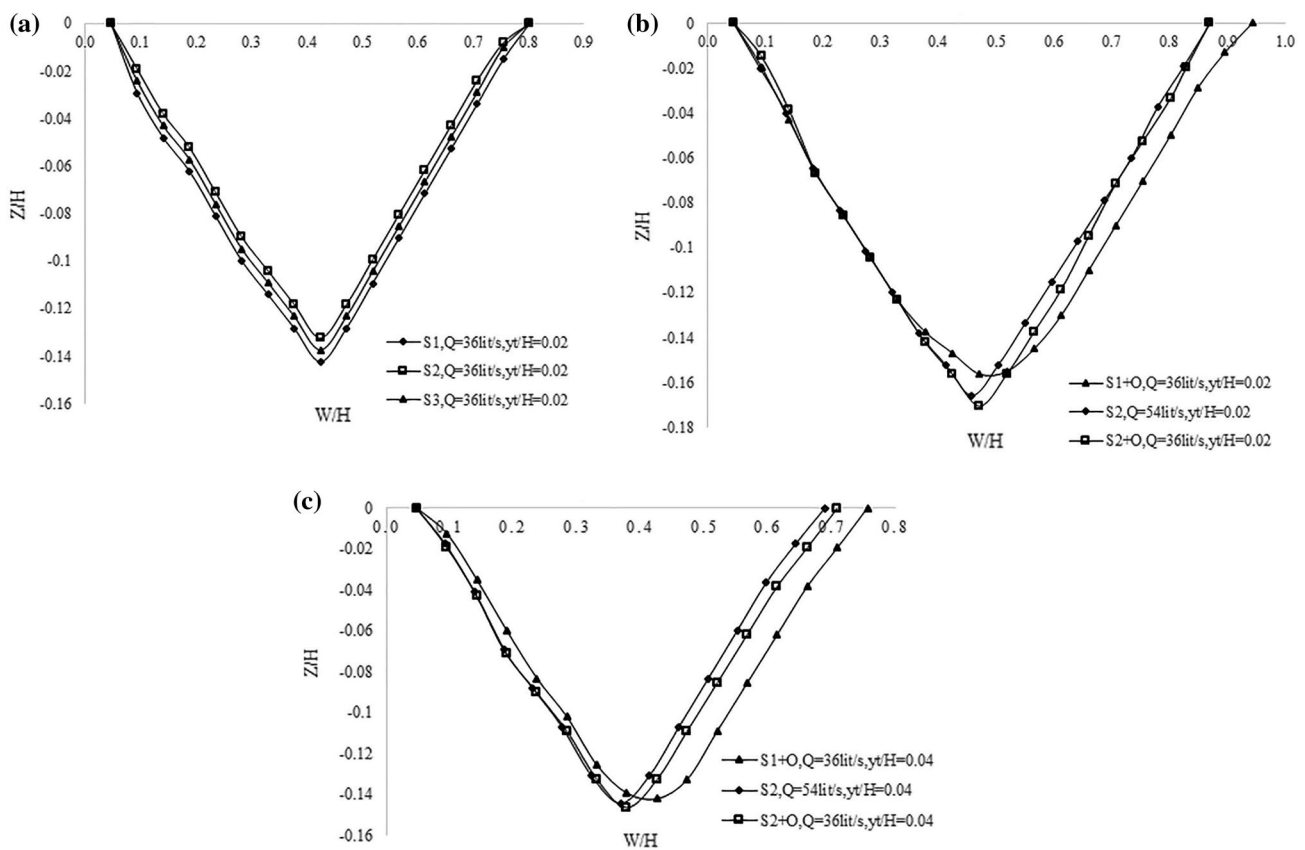


Fig. 10 Comparison of transverse scour profiles: **a** single spillway jet at discharge rate of 36 l/s and $(Yt/H)=0.02$; **b** coaxial and non-axial jets with discharge rate of 36 l/s of spillway and discharge rate of 18 l/s of orifice; **c** single jet of spillway at discharge rate of 54 l/s

subject requires additional experiments with different tail waters.

- Due to the similarity of the position of the gates 1 and 3, maximum scour depth and sedimentation in these two states are approximately equal to the combination with the orifice jet. On the other hand, the same applies to the spillway jets without orifice operation: the maximum depth of scour and deposition for spillway gates 1, 2, and 3 are roughly equal due to equal discharge rates and the same geometric characteristics.
- Non-dimensionalized results of the longitudinal scour profile using position and maximum scour depth indicates self-similarity of curves: it is possible to develop a single relation for the scour curve. Considering this non-dimensional profile, the length of the scour hole in the experiments of this research is independent of the tail water and the Froude number: the scour length is about one and a half times the corresponding position, and the maximum scour depth and hill length is about one to one and a half times the depth corresponding to the maximum scour depth.

The results of this studies show that if the outflow of dams can be divided between flood discharge structures such as spillway and orifice and thus form a combined outlet jet, downstream scouring problems will be reduced. In particular, the combination of jets in non-axial form will be more effective in reducing scouring. Future investigations should study more closely the impact of tail water on the operation of combined jets.

References

Aderibigbe O, Rajaratnam N (1996) Erosion of loose beds by submerged circular impinging vertical turbulent jets. *J Hydraul Res* 34(1):19–33

Almeida Manso PFD (2006) The influence of pool geometry and induced flow patterns on rock scour by high-velocity plunging jets. EPFL, Lausanne

Azmathullah H, Deolalikar P (2006) Estimation of scour below spillways using neural networks. *J Hydraul Res* 44(1):61–69

Canepa S, Hager WH (2003) Effect of jet air content on plunge pool scour. *J Hydraul Eng* 129(5):358–365. [https://doi.org/10.1061/ASCE0733-9429\(2003\)129:5\(358\)](https://doi.org/10.1061/ASCE0733-9429(2003)129:5(358))

- Chee SP, Kung T (1974) Piletas de derrubio autoformadas. 6th Latin American congress of the international association for hydraulic research, Bogata
- Dehghani AA, Bashiri H, Dehghani N (2010) Downstream scour of combined flow over weirs and below gates. In: River Flow 2010—Dittrich, Koll, Aberle & Geisenhainer (eds)
- Farhoudi J, Smith KVH (1985) Local scour profiles downstream of hydraulic jump. *J Hydraul Res IAHR* 23(4):343–358
- Khatsuria RM (2004) *Hydraulics of spillways and energy dissipators*. CRC Press
- Mehraein M (2012) Scour formation due to simultaneous circular impinging jet and wall jet. *J Hydraul Eng Res* 50(4):395–399
- Mih WC, Kabir J (1983) Impingement of water jets on nonuniform streambeds. *J Hydraul Eng* 109(4):536–548
- Negam AM (1995) Characteristics of combined flow over weirs and under gates with unequal contractions. In: *Advances in hydrosience and engineering*. March, Tsinghua University Press, Beijing, pp 285–292
- Pagliara S, Hager WH, Minor H-E (2006) Hydraulics of plane plunge pool scour. *J Hydraul Eng* 132(5):450e461. [https://doi.org/10.1061/ASCE0733-9429\(2006\)132:5\(450\)](https://doi.org/10.1061/ASCE0733-9429(2006)132:5(450))
- Pagliara S, Palermo M, Carnacina I (2011) Scour process due to symmetric dam spillways crossing jets. *Int J River Basin Manag* 9(1):31e42
- Pagliara S, Palermo M (2017) Scour process caused by multiple sub-vertical non-crossing. *Water Sci Eng* 10(1):17–24
- Rajaratnam N, Berry B (1977) Erosion by circular turbulent wall jets. *J Hydraul Res* 15(3):277e289. <https://doi.org/10.1080/00221687709499648>
- Sui J, Faruque M, Balachandar R (2008) Influence of channel width and tailwater depth on local scour caused by square jets. *J Hydro Environ Res* 2(1):39–45
- Uyumaz A (1988) Scour downstream of the vertical gate. *J Hydraul Eng* 114(7):811–816
- Veronese A (1937) Erosioni di fondo a valle di un scarico. *AnnLavori Pubblici* 75(9):717–726 (in Italian)